



ELSEVIER

Agricultural Systems 72 (2002) 215–239

 AGRICULTURAL
SYSTEMS

www.elsevier.com/locate/agsy

Error analysis of soil temperature simulations using measured and estimated hourly weather data with 2DSOIL

D.J. Timlin^{a,*}, Ya. Pachepsky^b, B.A. Acock^{a,1},
J. Šimunek^c, G. Flerchinger^d, F. Whisler^e

^aUSDA-ARS Alternate Crops and Systems Laboratory, Bldg 007, Rm 116,
10300 Baltimore Ave, Beltsville, MD 20705, USA

^bUSDA-ARS Hydrology Laboratory, Rm, 10300 Baltimore Ave, Beltsville, MD 20705, USA

^cUSDA/ARS US Salinity Laboratory, 450 W Big Springs Rd, Riverside, CA 92507-4617, USA

^dNorthwest Watershed Research Center, 800 Park Blvd, Suite 105, Boise, ID 83712-7716, USA

^eDepartment of Plant & Soil Sciences, Mississippi State University, PO Box 9555,
Mississippi State, MS 39762, USA

Received 6 September 2000; received in revised form 30 April 2001; accepted 29 May 2001

Abstract

Many crop simulation models use 1-h time steps for atmospheric, soil and plant processes but often meteorological data are only available as daily summaries. The objective of this study was to investigate how errors in estimation of hourly values of solar radiation and air temperature affect errors in simulation of soil temperature using the model 2DSOIL. 2DSOIL is a two-dimensional finite element model that simulates water flow, chemical, water and solute uptake by plant roots, chemical equilibria processes, and gas and heat transport in soil. The standard deviations of the differences between hourly estimated air temperatures were about 2°C and 85 W m⁻² for solar radiation. The mean difference in simulated and measured soil temperatures using measured hourly weather data for all depths at both sites was less than 1°C and standard deviations were about 1–3°C indicating low bias. The range of errors was highest in the surface soils when the soil was wetted after rainfall. Relative to simulated soil temperatures using measured hourly data, simulated soil temperatures using estimated data were, on average over all depths, 2°C lower and standard deviations ranged from 2 to 3°C. The errors were similar over all depths. Use of estimated hourly air temperature and radiation generally resulted in underpredictions of soil temperature by 2–3°C and increased error. Also maximum daily soil temperatures were underestimated. Published by Elsevier Science Ltd.

Keywords: 2DSOIL; Soil temperature; Simulation; Down scaling; Weather data

* Corresponding author.

¹ Present address: Adjunct Professor, Duke University Phytotron, Duke University, Durham, NC27708, USA.

E-mail addresses: dtimlin@asrr.arsusda.gov (D.J. Timlin).

Nomenclature

γ	psychrometric constant, $\text{kPa } (^\circ\text{C})^{-1}$
δ	solar declination
$\Delta\varepsilon$	vapor pressure deficit, kPa
θ	soil moisture content for the grid nodes at the soil surface
ν	humidity ratio
ν_s	albedo of soil
ε	actual water vapor pressure for day (assumed constant), kPa
$\varphi;$	local latitude $^\circ$
ε_s	saturation vapor pressure, kPa
ε_w	saturation vapor pressure at wet bulb temperature, kPa
a	atmospheric transmission coefficient
b_ε	slope of saturation water pressure curve, $\text{kPa } (^\circ\text{C})^{-1}$
E_s	potential evaporation rate from soil surface, cm day^{-1}
J	day of the year
L	latent heat of evaporation [$2500.8 - 2.37 (\text{Temperature})$], J g^{-1}
R	actual radiation incident at earth's surface, W m^{-2}
$R_{00,n}$	radiation incident at the top of the atmosphere at noon, W m^{-2}
$R_{0,n}$	potential radiation incident at earth's surface at noon, W m^{-2}
R_n	actual radiation incident at earth's surface at noon, W m^{-2}
R_{Ns}	net radiation on a bare soil surface, W m^{-2}
R_t	daily solar radiation integral W m^{-2}
R_u	net upward long wave radiation, W m^{-2}
T_a	air temperature, $^\circ\text{C}$
t_d	daylength, hours
t_{dk}	time of dusk, hours
T_{dk}	air temperature at dusk, $^\circ\text{C}$
t_{dn}	time of dawn, hours
T_{dry}	dry bulb temperature $^{-1} \text{ }^\circ\text{C}$
T_{max}	maximum air temperature during the day, $^\circ\text{C}$
t_{maxhr}	time of maximum air temperature measured from dawn, hours
T_{min}	minimum air temperature during the day, $^\circ\text{C}$
T_{mint}	minimum air temperature for the following day, $^\circ\text{C}$
T_{wet}	wet bulb temperature $^\circ\text{C}$
T_y	air temperature at sunset on the previous day, $^\circ\text{C}$
V	wind speed at 2 m height, km h^{-1}
H	sensible heat flux between the soil and air, $\text{J cm}^{-2} \text{ d}^{-1}$
G	net heat flux into or out of the soil, $\text{J cm}^{-2} \text{ d}^{-1}$
RN_{LS}	re-radiation of heat from the soil to the air ($\text{J cm}^{-2} \text{ d}^{-1}$)
H_{rain}	heat flux into the soil with rain ($\text{J cm}^{-2} \text{ d}^{-1}$)

Soil temperature is an important environmental variable for plant growth and development. Soil temperatures affect root growth (Koski et al., 1988), and biological processes such as nitrogen dynamics and pesticide transformation (Choi et al., 1988). Heat radiating from the surface soil impacts the crop canopy. Crop simulators must therefore be able to calculate soil temperatures accurately to be useful as crop management tools.

Many crop simulation models use 1-h time steps for atmospheric, soil and plant processes but often meteorological data are only available as daily summaries. Meteorological data that provide boundary conditions for soil temperature simulations typically include air temperature at 2 m, radiation, rainfall, and wind speed. Several procedures were suggested to downscale daily weather data to hourly values (i.e. Floyd and Braddock, 1984; Geng et al., 1985; Ephrath et al., 1996). These procedures were judged by the accuracy of estimating the weather variables per se.

Because of high nonlinearity and complexity of responses of biological systems to environmental variables, errors in input data can be magnified through the simulation progress. Such error propagation was observed in modeling studies with estimated soil hydraulic properties (Wösten and van Genuchten, 1988; Leenhardt, 1995). Because of error propagation, the accuracy of the input estimation per se does not tell what errors can be expected in simulation results of interest. Wösten and van Genuchten (1988) suggested that the prediction accuracy of the estimated soil parameters can be quantified in terms of the accuracy of hydrologic model output. Leenhardt (1995) noted that error propagation depends on the model in use, and therefore the estimation procedure has to be evaluated in the context of a specific model. The situation with using downscaled weather data in crop simulations bears a similarity to using estimated soil parameters. The procedures to downscale weather data should be judged by the accuracy of simulations carried out with a specific model.

A modular simulator of soil processes, 2DSOIL, has been developed from other models to be easily interfaced with crop models (Timlin et al., 1996). 2DSOIL is a two-dimensional finite element model that simulates water flow, chemical, water and solute uptake by plant roots, chemical equilibria processes, and gas and heat transport in soil. 2DSOIL has also a meteorological module to simulate hourly energy exchange at the soil–atmosphere interface that downscales daily summaries to hourly values. This meteorological module was adapted from the GLYCIM model (Acock and Trent, 1991) but never fully evaluated. The objective of this study was to evaluate this module in 2DSOIL using two criteria: a correspondence between measured and simulated hourly meteorological variables, and a correspondence between simulated and measured soil temperatures.

1. Materials and methods

1.1. Weather and soil temperature data

The weather and soil temperature data are from two experiments carried out on bare soil. The first data set was from in Pullman, WA (Flerchinger and Saxton,

1989). The soil is a Palouse silt loam (fine-silty mixed Mesic Pachic Ultic Haploxeroll). The soil temperature data were collected every 3 h at a conventionally tilled plot. The temperatures were not averaged over that period but “point” measurements were output. The measurement depths were surface (to 0.01 m), 0.076, 0.152, 0.254, 0.381, 0.533, 0.686, 0.838, 1.067, 1.372, and 1.676 m. The data were collected over the period from 1 March to 22 September 1987. The second data set was obtained from the Plant Sciences Research Center at Mississippi State University (Khorsandi et al., 1997). The soil was a Marietta loam (fine-loamy, siliceous, thermic Fluvaquentic Eutrochrept). Only daily average soil temperatures were available at this site although hourly soil temperatures were originally measured. Soil temperature was measured in ridge and furrow positions of a ridge tilled soil. The distance between furrows was 90 cm and the furrow height was 15 cm. Soil temperatures were measured to 60 cm depth and measurements were available at 0.05, 0.1, 0.25, and 0.6 m. The data are from the period 20 May to 27 September 1991. Soil hydraulic properties and hourly values of air temperature, solar radiation, and wind velocity were available at both sites.

2. The meteorological model

The model of soil–atmosphere interaction uses relationships of celestial geometry, crop canopy geometry, and radiation balance theory (Acock and Trent, 1991; Acock et al., 2000). The model here is described as a sequence of submodels. A description of the symbols and their units are listed in the Nomenclature. The time unit of variables that have a time component, for example evaporation rate, is day (d^{-1}). These are instantaneous rates of the variables, and these rates are updated on an hourly basis which is the time step of the meteorological module of 2DSOIL.

2.1. Incident radiation submodel.

Solar declination, δ , is calculated using the algorithm of Robertson and Russelo (1968)

$$\delta = \beta_1^+ \sum_{i=2}^{i=5} [\beta_i \sin(0.01721(i-1)J) + \beta_{i+4} \cos(0.01721(i-1)J)] \quad (1)$$

Here and below index i indicates that the value is valid over the hour centered at $t_i = (i-0.5)$ h and J is day of year. The coefficients β_i are equal to $\beta_1 = 0.3964$; $\beta_2 = 3.631$; $\beta_3 = 0.03838$; $\beta_4 = 0.07659$; $\beta_5 = 0.0$; $\beta_6 = -22.97$; $\beta_7 = -0.3885$; $\beta_8 = -0.1587$; $\beta_9 = -0.01021$.

Daylength, t_d is defined as the interval between sunrise and sunset; at both of these times the center of the sun’s disk is 50% below the horizon. The equation relating solar altitude and declination to latitude and hour (Smithsonian Meteorological Tables, 1966, p. 495) is solved for the hour angle and then results are converted to hours from solar noon. Doubling the answer gives day length:

$$t_d = \frac{\pi}{24} \arccos\left(-\frac{0.014544 + \sin\varphi\sin\delta}{\cos\varphi\cos\delta}\right) \quad (2)$$

with φ , latitude, in degrees.

The equations for solar radiation incident on top of the earth's atmosphere, $R_{00,n}$, are given in the Smithsonian Meteorological Tables (1966, p. 417). The conditional solar constant, i.e. the radiation flux on the top of the troposphere is assumed to be 1325.4 W m^{-2} (Budyko, 1974):

$$R_{00,n} = 1325.4 \frac{\cos(\varphi - \delta)}{Z^2} \quad (3)$$

where $Z = 1 + 0.01674 \sin[0.01721(J - 93.5)]$, is the radius-vector of the earth.

The atmospheric transmission coefficient, a , is estimated for different latitudes and times of year from the data of Budyko (1974):

$$\begin{aligned} a &= 0.68 + (1.57\xi - 0.1) \frac{145 - J}{1000}, & J \leq 145 \\ a &= 0.68 + [\xi(2.04 - 0.37\xi) - 0.19] \frac{J - 237}{1000}, & J \geq 237 \\ a &= 0.68 & 145 \leq J < 237 \end{aligned} \quad (4)$$

where $\xi = \varphi/30$.

Estimated potential radiation incident on the earth's surface at noon $R_{0,n}$, (W m^{-2}) is calculated as

$$R_{0,n} = \frac{1}{2} R_{00,n} \left(0.93 - \frac{0.02}{\cos(\varphi - \delta)} + a^{1/\cos(\varphi - \delta)} \right) \quad (5)$$

This equation was derived from an equation given in the Smithsonian Meteorological Tables (1966, p. 420). The adsorption of the extraterrestrial radiation is allowed to vary with atmospheric path length, i.e. solar altitude, according to the data given by Miller (1981).

Estimated actual radiation incident at the earth's surface at noon, R_n , (W m^{-2}) under a cloudless sky is calculated from the total measured daily radiation, R_t , (W m^{-2}) and the assumption that the radiation flux density varies as a half sine wave over the photoperiod:

$$R_n = \frac{\pi R_t}{t_d 2} \quad (6)$$

Both time of dawn, t_{dn} , and time of dusk, t_{dk} , are derived from daylength, t_d :

$$t_{dn} = 12 - t_d/2, \quad t_{dk} = 12 + t_d/2 \quad (7)$$

Actual radiation incident at the earth's surface at time t_i , R_i , (W m^{-2}) is calculated according to the half sine wave pattern:

$$R_i = R_n \sin\left(\frac{\pi(i - 0.5)}{t_d}\right) \quad (8)$$

Corrections are made for incomplete hours after dawn and before dusk to obtain hourly values.

2.2. Temperature–vapor pressure submodel

The time of maximum air temperature, measured from dawn (t_{dn}), is:

$$t_{\text{maxhr}} = \frac{t_d}{\pi} \left[\pi - \arcsin\left(\frac{T_{\text{max}}}{R_n(0.0945 - 8.06 \cdot 10^{-5} R_n + 6.77 \cdot 10^{-4} T_{\text{max}})}\right) \right] \quad (9)$$

where the expression after 'arcsin' is less than one. The coefficients were fit to data from Mississippi (Acock and Trent, 1991). The air temperature at sunset is:

$$T_{dk} = \frac{T_{\text{max}} - T_{\text{min}}}{2} \left[1 + \sin\left(\frac{\pi t_d}{t_{\text{maxhr}}} + \frac{3\pi}{2}\right) \right] + T_{\text{min}} \quad (10)$$

Diurnal temperature variation is approximated by a half sine wave during the day and by either a logarithmic or a linear dependency at night. At time $t = t_i$ we have:

$$\begin{aligned} T_{a,i} &= T_{\text{min}} + \frac{T_{\text{max}} - T_{\text{min}}}{2} \left[1 + \sin\left(\frac{\pi(t_i - t_{dn})}{t_{\text{maxhr}}} + \frac{3\pi}{2}\right) \right], t_{dn} \leq t_i \leq t_{dk}, \\ T_{a,i} &= T_{\text{min}} + T_* \left[\left(1 + \frac{T_y - T_{\text{min}}}{T_*}\right)^{\frac{t_{dn} - t_i}{2t_{dn}}} - 1 \right], t_i < t_{dn}, T_y > T_{\text{min}}, \\ T_{a,i} &= T_{\text{min}} + (T_y - T_{\text{min}}) \frac{t_{dn} - t_i}{2t_{dn}}, t_i < t_{dn}, T_y \leq T_{\text{min}}, \\ T_{a,i} &= T_{dk} + T_* \left(1 + \frac{T_{dk} - T_{\text{mint}}}{T_*}\right) \left[\left(1 + \frac{T_{dk} - T_{\text{mint}}}{T_*}\right)^{-\frac{t_i - t_{dk}}{2(24 - t_{dk})}} - 1 \right], \\ t &> t_{dk}, T_{\text{mint}} < T_{dk}, \\ T_{a,i} &= T_{dk} + (T_{\text{mint}} - T_{dk}) \frac{t_i - t_{dk}}{2(24 - t_{dk})}, t_i > t_{dk}, T_{\text{mint}} \geq T_{dk} \end{aligned} \quad (11)$$

These equations have given a good fit to data sets from Arizona and Mississippi, when the parameter T_* was set at 5°C (Acock and Trent, 1991).

Calculations of water vapor pressure for the day depend on the availability of wet and dry bulb temperature values. If those are not available, dew point temperature is assumed to be the minimum temperature. When wet and dry bulb temperatures are

not known, the algorithm of Weiss (1977) is used to calculate water vapor pressure, ε , where T_{\min} is used for the dew point temperature:

$$\varepsilon = 0.61 \exp\left(\frac{17.27 T_{\min}}{T_{\min} + 237.3}\right) \quad (12)$$

The psychrometric “constant”, γ is $0.0645 \text{ kPa } ^\circ\text{C}^{-1}$.

If wet and dry bulb temperatures are known, then calculations for the water vapor pressure, ε , include the value of the saturation vapor pressure at wet bulb temperature ε_w , humidity ratio ν , and latent heat of evaporation L (J g^{-1}):

$$\begin{aligned} \varepsilon_w &= 0.61 \exp\left(\frac{17.27 T_{\text{wet}}}{T_{\text{wet}} + 237.3}\right); \nu = \frac{0.622 \varepsilon_w}{101.3 - \varepsilon_w}; \\ L &= 2500.8 - 2.37 T_{\text{wet}}; \gamma = 62.81 \frac{1.006 + 1.846 \nu}{L(0.622 + \nu)^2}; \\ \varepsilon &= \varepsilon_w - \gamma(T_{\text{dry}} - T_{\text{wet}}) \end{aligned} \quad (13)$$

The saturation vapor pressure, ε_s is calculated using air temperature (T_a). The slope, b_{ε_s} , of the saturation water vapor pressure curve is estimated using the value of the saturated vapor pressure, and finally, the vapor pressure deficit, $\Delta\varepsilon$, is then calculated from:

$$\begin{aligned} \varepsilon_s &= 0.61 \exp\left(\frac{17.27 T_a}{T_a + 237.3}\right) \\ b_{\varepsilon} &= 0.61 \exp\left(\frac{17.27(T_a + 1)}{(T_a + 1) + 237.3}\right) - \varepsilon_s \\ \Delta\varepsilon &= \varepsilon_s - \varepsilon \end{aligned} \quad (14)$$

Where ε is from Eq. (11) or Eq. (12) depending on the availability of wet and dry bulb temperatures.

2.3. Potential evapotranspiration submodel

The evapotranspiration submodel is based on the Penman (1963) equation. Net upward long-wave radiation, R_u , is calculated using an approximation derived by Linacre (1968). Linacre’s original approximation used the ratio of the mean number of hours of bright sunshine to day length. This ratio has been replaced by the ratio of actual radiation at the earth’s surface at solar noon to the potential radiation. Longwave radiation is calculated for each period of the day, t_b , where radiation is greater than zero using air temperature (T_a) at that time:

$$R_u = 11.2 \times (100 - T_a) \frac{R_n}{R_{0,n}} \quad (15)$$

The albedo (α) of exposed soil is estimated from the data of Bowers and Hanks (1965) as a function of soil water content of the surface soil (θ):

$$\alpha = 0.3 - 0.5\theta \quad (16)$$

Net radiation on the soil surface (R_{Ns}) for the time period, t_i , is calculated from albedo (α), net upward longwave radiation (R_u) and estimated actual radiation incident at the earth's surface [Eq. (8)]:

$$R_{Ns} = (1 - \alpha)R_i - R_u \quad (17)$$

Penman's equation gives the potential evaporation rate from the soil, E_s ($\text{g cm}^{-2} \text{ day}^{-1}$), for time period, t_i :

$$E_s = \frac{24 \frac{b_\epsilon}{\gamma} \frac{3600}{L} R_{Ns} + 109.375(1 + 0.419V)\Delta\epsilon}{\frac{b_\epsilon}{\gamma} + 1} \quad (18)$$

The actual evapotranspiration will be determined by 2DSOIL using an iterative process that depends on the current water content and transport properties of the soil.

2.4. Boundary condition for the heat transport in soil

The heat balance at the soil surface is:

$$-G = L \cdot E_s + R_{Ns} + H \quad (19)$$

Here, L is the latent heat of vaporization of water (J g^{-1}), E_s is evaporation rate ($\text{g cm}^{-2} \text{ day}^{-1}$), R_{Ns} is the radiant energy flux ($\text{J cm}^{-2} \text{ day}^{-1}$), H is sensible heat flux ($\text{J cm}^{-2} \text{ day}^{-1}$) between the soil and air and G is the net heat flux into or out of the soil ($\text{J cm}^{-2} \text{ day}^{-1}$). Units for heat are given as Joules in this section since these are the units used in the soil module.

Sensible heat flux (H) is calculated as a function of the temperature difference between the soil surface and the air. For bare soil, the sensible heat transfer between the soil and atmosphere occurs when a temperature difference exists between the soil surface and air and the soil surface is warmer than the air:

$$H = (24.1 + 8.38V) \cdot (T_a - T_{\text{surf}}) \quad (20)$$

Here the expression for the coefficient of heat conduction between the soil and the atmosphere is from Linacre, (1968, Appendix 2), V is windspeed at 2 m (km day^{-1}), T_a is air temperature and T_{surf} is soil surface temperature. When the temperature of the soil is greater than the temperature of the air, some heat is re-radiated as long

wave radiation into the atmosphere, RN_{LS} (Linacre, 1968). This re-radiation becomes a component of H in Eq. (19). Re-radiation of heat from the soil to the air (Linacre, 1968, uses $\text{cal cm}^{-2} \text{min}^{-1}$) is calculated as (Linacre, 1968):

$$RN_{LS} = (0.00683 + 0.00009 \cdot T_a) \cdot (T_a - T_{\text{surf}}) \quad T_{\text{surf}} > T_a \quad (21)$$

The units of RN_{LS} are then converted to $(\text{J cm}^{-2} \text{day}^{-1})$.

Heat influx, H_{rain} ($\text{J cm}^{-2} \text{day}^{-1}$) due to rainfall is calculated based on the intensity of rainfall and temperature of the rainwater (the latter assumed to be equal to the air temperature):

$$H_{\text{rain}} = I_R C_W (T_a - T_{\text{surf}}) \quad (22)$$

where I_R is rain intensity, $\text{g cm}^{-2} \text{day}^{-1}$, and C_W is the specific heat capacity of water, $\text{J g}^{-1} (\text{°C})^{-1}$.

3. Boundary conditions, and water flow and heat transport parameters in 2DSOIL

2DSOIL is a finite element representation of matter and energy transport in soil. The model uses adaptive time steps (Timlin et al., 1998). The minimum time step depends on either convergence criteria for the iterative equations or the amount of time that needs to pass before a boundary condition is updated. The default units of the time step can be any time value but all the parameters and coefficients must use the same unit. For the simulations in this paper, a time unit of day is used. Radiation or potential evapotranspiration are updated each hour or 1/24 of a day. The shorter the time period between updates, the more accurate will be the information passed to the model, however, more detailed information would be required.

The hydrology and heat transport components of 2DSOIL require, as input, soil hydraulic parameters, the saturated soil hydraulic conductivity, K_{sat} (cm day^{-1}), moisture retention parameters, saturated water content, soil texture, and initial water contents and temperatures. The soil hydraulic properties are described by the van Genuchten equation (van Genuchten, 1980), calculations of thermal conductivity are from DeVries (1963), water flow and heat transport are calculated using a two-dimensional finite element representation of the Richards equation (Šimůnek et al., 1994). All parameters for the model were chosen from the literature or calculated from measured data.

The soil hydraulic properties for the Washington site included the saturated hydraulic conductivity and Brooks-Corey parameters for the matric potential vs. water content relationship. At the Mississippi site, saturated hydraulic conductivity and measured values of matric potential and water content were available. van Genuchten's equation (van Genuchten, 1980) for moisture release and unsaturated hydraulic conductivity was fitted to the data. Parameters of the equation, along with soil texture and saturated hydraulic conductivity are given in Table 1.

Table 1
Soil properties used for the Washington and Mississippi sites^a

Depth (m)	Ksat	θ_s^b (cm ³ cm ⁻³)	θ_r^{cd} (cm ³ cm ⁻³)	α^d (cm ⁻¹)	n^d	ϕ_b (Mg m ⁻³)	Sand and silt (kg kg ⁻¹)	Clay (kg kg ⁻¹)	Organic matter (kg kg ⁻¹)
<i>Washington</i>									
0.000–0.076	2.88	0.588	0.095	0.0129	1.440	0.95	68.1	0.301	0.018
0.077–0.152	2.88	0.481	0.078	0.0129	1.440	0.95	68.2	0.302	0.015
0.153–0.254	2.88	0.517	0.067	0.0257	1.399	1.26	68.5	0.305	0.010
0.255–0.381	3.84	0.465	0.074	0.0302	1.336	1.17	68.8	0.308	0.005
0.382–0.533	6.72	0.508	0.072	0.0427	1.330	1.32	69.0	0.310	0.001
0.534–0.686	5.04	0.478	0.070	0.0339	1.353	1.21	69.0	0.310	0.001
0.687–0.838	3.36	0.440	0.065	0.0271	1.362	1.29	72.0	0.280	0.001
0.839–1.067	2.30	0.404	0.061	0.0219	1.388	1.39	72.0	0.280	0.001
1.068–1.372	0.27	0.367	0.069	0.0154	1.399	1.49	76.0	0.240	0.001
1.373–1.676	0.07	0.338	0.074	0.0109	1.389	1.59	76.0	0.240	0.001
<i>Mississippi</i>									
0.000–0.200	12.64	0.540	0.167	0.2894	1.326	1.40	77.0	0.210	0.020
0.201–0.900	15.11	0.442	0.201	0.3714	1.237	1.60	69.0	0.300	0.010
0.901–2.050	1.59	0.435	0.226	0.4442	1.226	1.40	68.0	0.315	0.005

^a The values θ_s , θ_r , α , and n are parameters for the van Genuchten equation (van Genuchten, 1980), and ϕ_b is bulk density.

^b Saturated water content.

^c Residual water content.

^d Parameters for van Genuchten's equation.

The bottom boundary for water flow was given as a free drainage condition, i.e. flux out the bottom boundary was equal to the unsaturated hydraulic conductivity at the current matric potential (unit gradient). In absence of other information, a constant boundary value of 20°C was used for temperature at the Mississippi site. A time varying boundary condition was used at the Washington site. This boundary condition was used at the Washington site since the temperatures at the 1.67 m depth showed more variation over time than did the temperatures at the Mississippi site. The temperature at the bottom boundary was set to the temperatures at the 1.67 m depth. Water and heat flow are not coupled in 2DSOIL, and there is no provision for vapor flux.

4. Design and sequence of the simulations

Hourly values of temperature, radiation and wind velocity were calculated from daily weather data (total radiation, maximum and minimum temperatures, and daily windrun) to evaluate the model used to estimate hourly meteorological data from daily summary data. In the second step, simulations of soil temperature were run using measured hourly weather data as input. The measured soil temperature data are point (instantaneous) measurements at Washington and averages of temperature over 24 h at Mississippi. Instantaneous temperatures were output for the Washington data and daily averages for the Mississippi data. These averages were compared to the measured temperatures. In order to evaluate errors of simulated soil temperatures, soil temperatures were also simulated using estimated hourly meteorological data. These simulations were carried out the same as the simulations using measured hourly data. The comparison of simulation and measurements was carried out for a long time sequence of measured values, 195 days for Washington and 100 days in Mississippi.

A bare, flat soil surface was simulated for the Washington site. A bare, ridge and furrow surface configuration was used for the Mississippi site. No calibrations of 2DSOIL were made prior to the temperature simulations.

Relative error was used to compare errors in simulations of soil temperatures using measured and estimated hourly weather data. Relative error was defined as the difference in soil temperatures simulated using measured hourly data, and soil temperatures simulated using estimated hourly values divided by soil temperatures simulated using measured hourly data.

5. Results and discussion

5.1. Comparison of measured and calculated hourly air temperatures and solar radiation

Measured hourly radiation and air temperature, and hourly values calculated from daily weather data for both Washington (Fig. 1) and Mississippi (Fig. 2) have

similar diurnal distributions throughout the 24-h period. Measured solar radiation for the five day period shown in Figs. 1 and 2 appears higher than predicted at midday for both sites. The differences in radiation as a function of time of day were similar for both locations (Table 2). The differences seen at the peak radiation at noon are noticeable because the measured radiations are somewhat larger than the calculated radiations during most of the daylight hours. The mean differences in solar radiation (measured–predicted) for all the data given in Table 2 were consistently positive from about 11:00 until 18:00 h and increased to about $+90 \text{ W m}^{-2}$ at midday (Table 2). The differences were consistently negative before 11:00 h. The positive differences, however are largely within the standard deviations of the mean differences. The consistent positive differences do suggest a slight bias. The magnitudes of the predicted and measured temperatures at a particular time could be

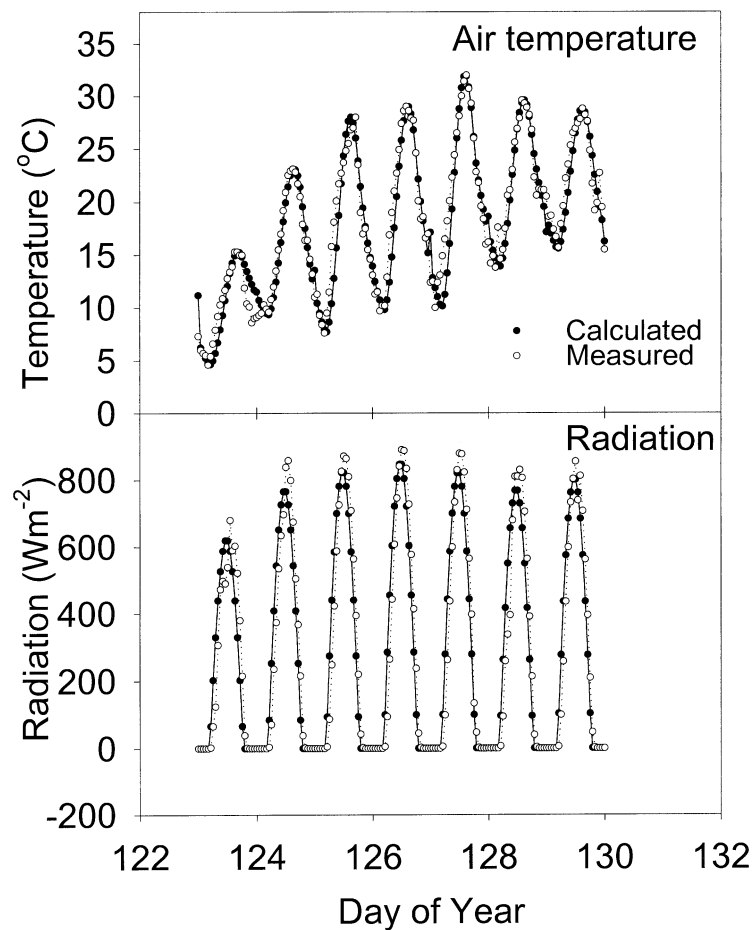


Fig. 1. Measured and calculated hourly air temperature, and radiation for the Washington site for a selected period of 7 days.

different by as much as 5–10°C and radiation by as much as 500 W m⁻² (Fig. 3) over all the data.

The calculated air temperatures in the morning hours at both sites were, on average, lower than measured temperatures (Table 2). The mean bias in air temperatures was greater for the Washington site than for the Mississippi site. The standard deviations were comparable for the two sites, however and the differences for most times of day were largely within the range of the standard deviations. The differences between the measured and calculated hourly temperatures for the Mississippi site between the hours of 13:00 to 14:00 were larger than the standard deviation. The data in Fig. 2 for a 5-day period suggest that the actual temperatures were rising at a slower rate than the calculated temperatures so that the calculated late-morning, early afternoon air temperatures became higher than measured. The reason for this

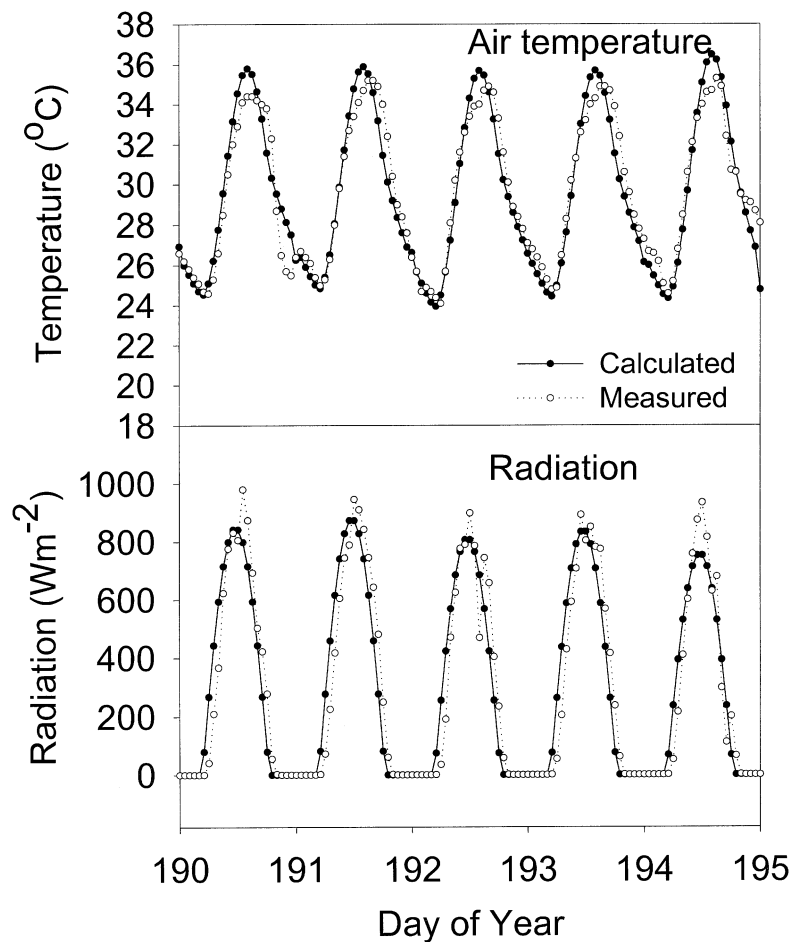


Fig. 2. Measured and calculated hourly air temperature, and radiation for the Mississippi site for a selected period of 7 days.

leveling off of temperature rise can be attributed to more efficient mixing of heated air from the ground level into the atmospheric boundary layer (Driedonks, 1981; Ephrath et al., 1996). This can affect the time of the maximum temperatures. Ephrath et al. (1996) reported that a sine-exponential model did not accurately predict the diurnal variation in air temperature. This was because maximum air temperature often occurred later than solar noon. They used a site specific parameter to lag temperature with respect to time. Our approach was similar here [Eq. (9)] with respect to calculating the time of maximum temperature.

Eq. (9) did give reasonable average estimates of the time of maximum temperatures for both sites. The observed times of maximum temperatures were highly variable, however and were probably affected by meteorological events such as weather fronts (Ephrath et al., 1996). This equation was developed for application of the GLYCIM model to conditions in Mississippi, USA (Acock and Trent, 1991) but

Table 2

Means and standard deviations (S.D.) of differences between measured and calculated hourly temperatures and radiation for the Washington ($n=196$ per hour) and Mississippi ($n=128$ per) sites as a function of hour of day^a

Site	Hour of day	Temperature (°C)		Radiation (W m ⁻²)	
		Mean	S.E.	Mean	S.D.
<i>Washington</i>					
	7	2.3	1.88	-170.1	69.84
	8	2.6	2.10	-148.5	81.78
	9	2.5	2.03	-101.5	87.31
	10	2.0	1.90	-46.6	99.51
	11	1.3	1.68	7.0	93.27
	12	0.6	1.34	51.1	97.37
	13	0.0	1.20	89.2	103.80
	14	-0.4	1.22	95.8	95.51
	15	-0.6	1.39	90.6	107.54
	16	-0.7	1.71	96.2	99.57
	17	-0.5	2.07	94.8	81.79
	18	-0.7	2.34	92.9	69.51
<i>Mississippi</i>					
	7	0.5	0.80	-187.5	60.47
	8	0.7	1.11	-153.4	85.88
	9	0.7	1.37	-83.9	90.52
	10	0.3	1.36	-10.8	111.83
	11	-0.3	1.23	24.4	128.51
	12	-0.9	0.91	77.0	126.47
	13	-1.4	0.85	83.3	144.71
	14	-1.5	1.23	88.6	133.51
	15	-1.1	1.20	78.9	135.14
	16	-0.6	1.65	85.1	125.21
	17	0.1	2.25	78.3	97.38
	18	0.6	2.16	76.7	55.34

^a Calculated values are obtained from Eqs. (1)–(14).

was never evaluated for other conditions. A replacement for this equation could be incorporated into 2DSOIL using the method of Eprath et al. (1996). The inability to simulate the percentage and timing of cloud cover will also add to the error. Cloud cover will reduce the daily radiation integral however which allows some compensation.

Fig. 3 shows the distributions of the bias errors (measured- calculated) for the two sites. The ranges in error were similar for the two sites for either air temperature or

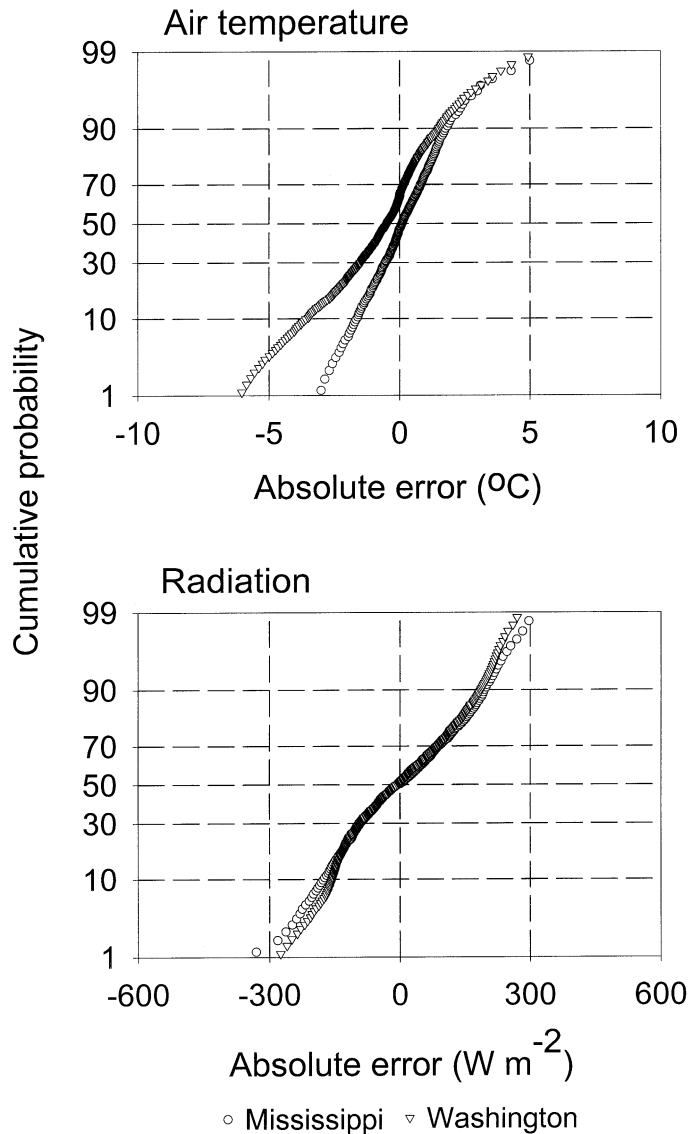


Fig. 3. Cumulative probabilities distributions of errors (bias) in calculated air temperatures and radiation for the two sites. Absolute error (bias error) is defined as measured-calculated temperature or radiation.

radiation. The error bias is larger for radiation than for air temperatures, however. For all times of the day, 35% of the errors are positive for the Washington site and 53% for the Mississippi site. The errors in radiation are more evenly distributed about zero than for temperature.

6. Soil temperature simulations using measured hourly air temperatures and radiation

Simulated soil temperatures from the Washington site capture the measured relative changes in soil temperature with time and depth (Fig. 4). The differences between simulated and measured soil temperatures were generally larger during the daylight hours than during the evenings. During several time periods, however, the measured temperatures in the surface soil were as much as 15–20°C larger than the simulated temperatures (Fig. 4b). The largest differences occurred during or immediately after days where there was rainfall. Similar differences in temperature are seen for deeper layers of the profile.

The mean differences between measured and simulated soil temperatures for all depths at the Washington site were all less than the standard deviation (Table 3). The standard deviation for the mean difference was largest at the surface but similar for the other depths. Overall there is no significant bias in the simulated temperatures and the standard deviation is in the range of 1–2°C. The larger range of temperatures in the soil surface contributes to the increased error there.

There is a diurnal pattern to the errors for soil temperature simulations at the Washington site as a function of DOY for the surface layer and 0.15 m depth (Fig. 5). The diurnal error indicates that the simulated soil temperatures were lower than measured temperatures during the day and slightly higher during the night.

Table 3

Summary statistics for differences between measured and simulated soil temperatures (°C) at 10 depths at the Washington site ($n = 1523$ per depth)^a

Depth	Mean difference	Maximum	Minimum	S.D.	R^2
0	-0.22	19.8	-11.9	5.29	79
0.076	0.29	8.4	-6.3	1.90	95
0.152	0.51	6.3	-5.8	1.89	94
0.254	0.53	6.1	-4.8	1.77	93
0.381	0.28	5.4	-4.4	1.55	94
0.533	0.26	5.1	-3.2	1.25	96
0.686	-0.04	4.5	-3.4	1.20	95
0.838	-0.21	3.6	-3.3	1.12	95
1.067	-0.48	2.9	-3.4	1.00	95
1.372	-0.54	1.9	-2.8	0.81	96
1.676	-0.54	1	-2.2	0.63	98

^a S.D. is standard deviation of the differences.

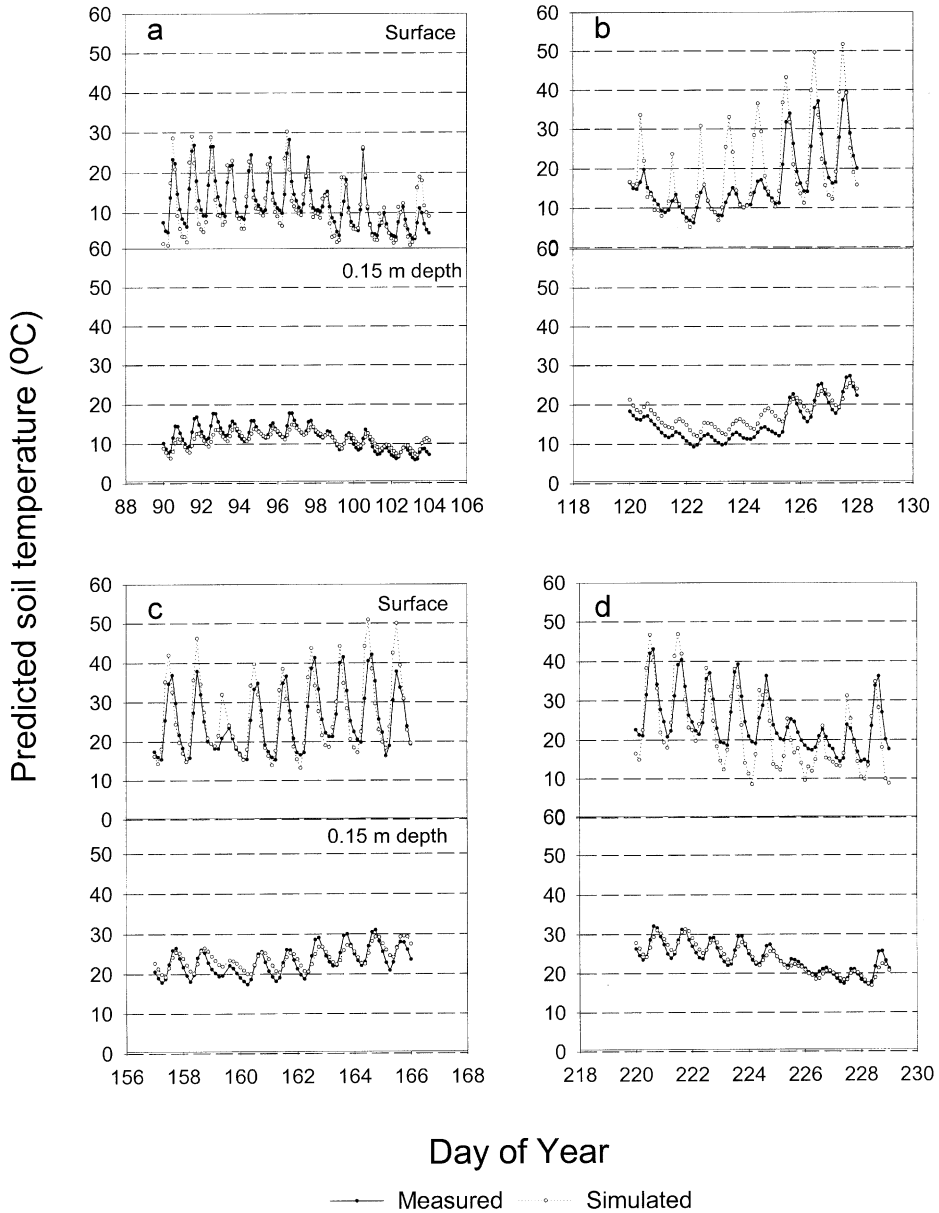


Fig. 4. Simulated and measured soil temperatures for the surface 0.01 and 0.15 m depths at Washington for 4-time periods: (a) DOY 88–105, (b) DOY 118–130, (c) DOY 156–168, and (d) DOY 218–230. Soil temperatures were simulated by 2DSOIL using measured hourly weather data.

These data represent a period with the largest errors for the entire period of simulations. One contributing factor to the errors may be the difference in the location of the measurement instrument and the depth the simulation results were recorded. There are large gradients in temperature at the soil surface and small differences in sensor placement can result in large differences in measured temperature. The first layer in the simulation extended from the surface to 0.02 m. Compared to a sensor in the first cm of soil, the simulated values in the 0–0.02 m depth may have been more damped during the hottest part of the day when the soil was very wet and lost heat faster in the evening. Also, the surface soil 0.01 m was quite variable in terms of meteorological conditions.

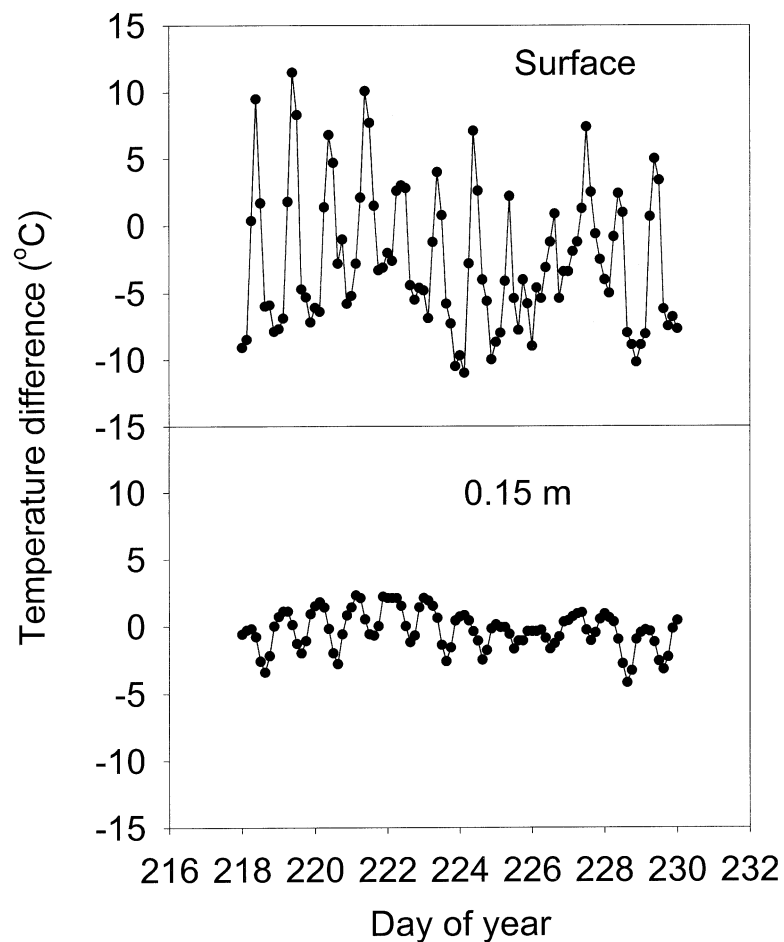


Fig. 5. Differences between measured and simulated temperatures at the Washington site as a function of time for a selected period of 13 days for the soil surface and 0.15 m depth. Soil temperatures were simulated by 2DSOIL using measured hourly weather data.

The weather measurement interval and method may also contribute to error. The soil temperature measurements at the Washington site represented instantaneous values while the input weather data was averaged over 1 h. The averaging of weather data results in the loss of information regarding the peak temperature and radiation occurring over the time of measurement. The high measured soil temperatures may have been in response to a very short period of high solar radiation.

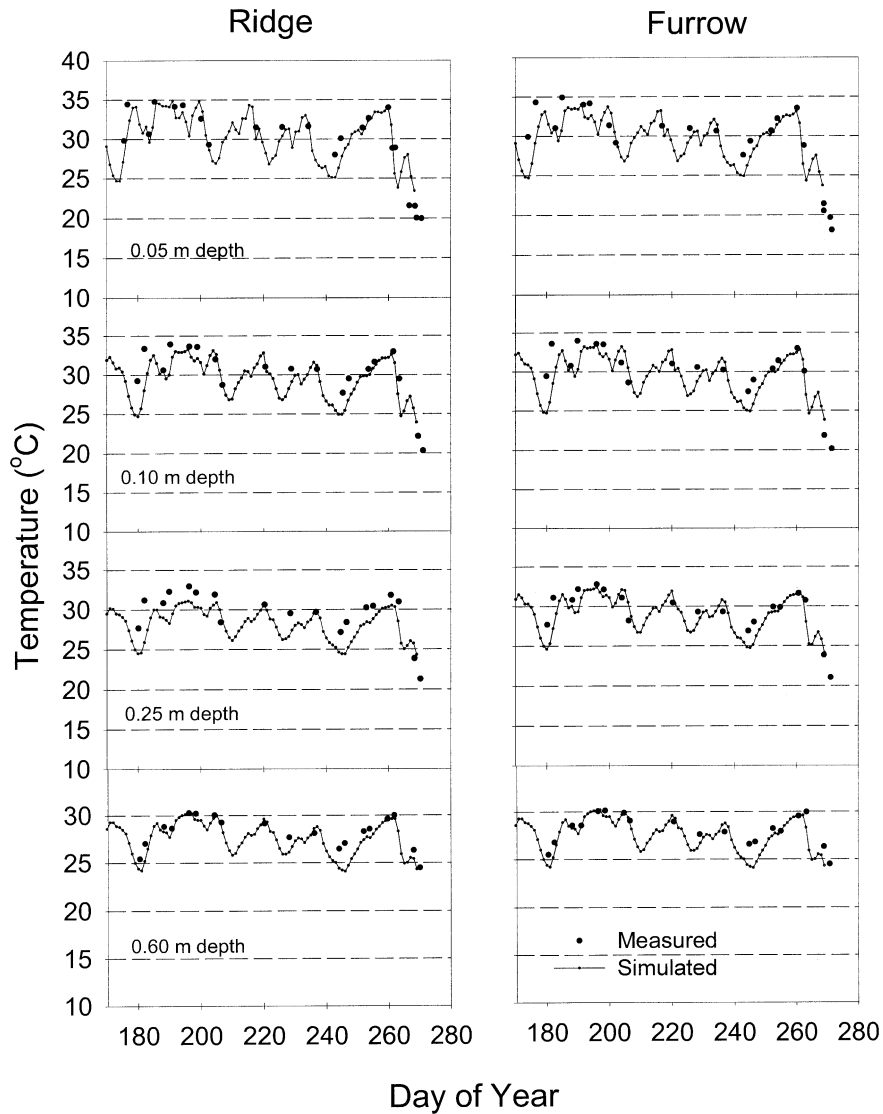


Fig. 6. Simulated and measured soil temperatures at Mississippi site for the ridge and furrow zones. Soil temperatures were simulated by 2DSOIL using measured hourly weather data.

Simulations by 2DSOIL gave reasonable results for simulated temperatures for the ridges and furrows for Mississippi (Fig. 6). There is minimal bias in the simulated temperatures for the Mississippi site, the mean differences are all less than 1°C and all less than the standard deviation (Table 4). There are no large differences among the errors for the four depths. The standard deviations, however were larger for the Mississippi data than for the Washington data. This reflects the smaller number of data for the Mississippi site. The ranges of differences for the two sites are similar (Tables 3 and 4). There was less error for the 0.05 m depth at Mississippi than for the 0.01 m depth at Washington.

Some errors in simulated temperature values may occur when the evaporation process begins to slow as the surface soil dries. This is due to the method 2DSOIL uses to determine the boundary condition when simulating surface soil drying. Evaporation from a wet soil will initially occur as a constant flux condition using the evaporation rate as a prescribed flux. If, during an iteration, the surface node cannot support the prescribed flux, the boundary condition is changed to a constant head. The value of the soil matric potential at this constant head is an input datum and approximates the matric potential at air dry water content. When the model switches to a constant head boundary condition, the actual rate of water loss from the surface cell is less than the potential rate given as the evaporation rate. Energy not used to evaporate water then goes to heat the soil. The true matric potential at which the evaporation becomes flux limited is difficult to determine from the available data. The evaporation rate is a function of the radiative demand as well as surface water content. It is more likely that errors will be larger between simulated and measured values when the evaporation process is in this transition phase. Once the soil dries the simulated and measured temperatures became more similar.

Table 4
Summary statistics for differences between measured and simulated soil temperatures at the Mississippi site ($n = 19$ per depth)^a

Row position	Depth (m)	Mean difference (°C)	Maximum	Minimum	S.D.
<i>Furrow</i>					
	0.05	0.8	5.2	-4.0	2.68
	0.10	0.8	5.1	-3.7	2.48
	0.25	0.7	3.9	-2.3	1.87
	0.60	0.7	2.7	-0.7	0.93
<i>Ridge</i>					
	0.05	0.7	5.1	-3.7	2.67
	0.10	0.4	4.5	-3.2	2.49
	0.25	0.5	3.5	-2.2	1.93
	0.60	0.2	2.6	-1.4	1.10

^a S.D. is standard deviation of the differences.

7. Simulated soil temperatures using calculated hourly air temperature and radiation

Use of hourly air temperatures and radiation that are calculated from max-min air temperatures and daily radiation integrals can potentially introduce additional errors into temperature simulations. Fig. 7 shows the cumulative probability of relative error for the Washington soil temperatures. The relative error ranges from –200 to 64% although only 35 out of 1500 values have relative errors more than the absolute value of 50%. More than 70% of the relative errors are greater than zero which means the simulated soil temperatures using calculated data are largely underestimated. Generally, soil temperatures in the higher range are underestimated for simulations with calculated hourly weather data. This is probably related to the underestimation of hourly radiation.

Table 5 lists the average differences between measured and simulated soil temperatures and standard deviations for the Washington data by depth. The mean differences as a function of depth were not large and varied from 1.7 to 2.5°C. The differences also increased slightly with depth. The data indicate a slight bias in the simulated temperatures when calculated hourly weather data are used because soil temperatures were underestimated by 1–2°C. The standard deviations for the mean differences between temperatures simulated using measured and calculated hourly

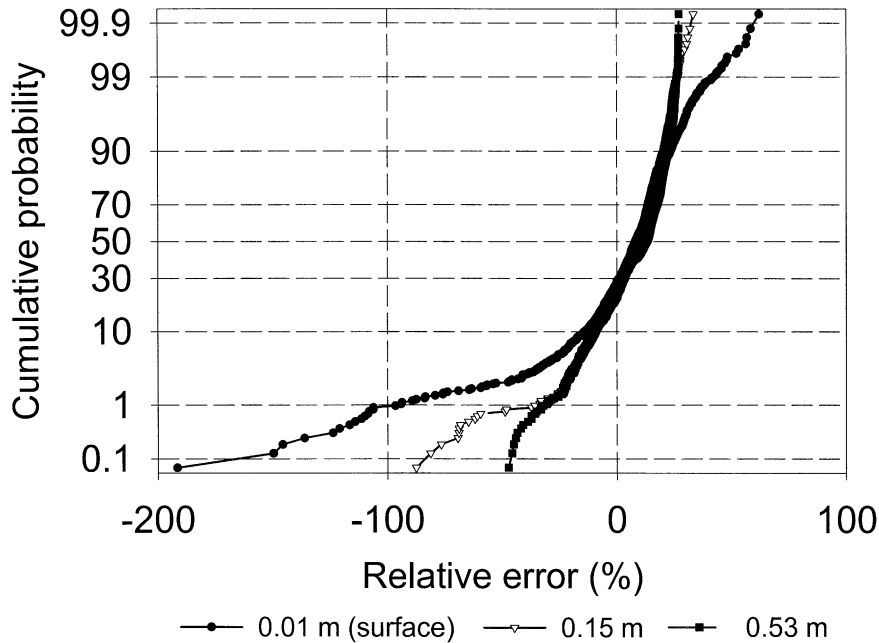


Fig. 7. Cumulative probability distribution of relative errors in simulated soil temperatures at Washington using measured and calculated hourly weather data for the surface 0.01, 0.15 and 0.53 m depths. Relative error is calculated as (simulated with measured hourly–simulated with calculated hourly)/simulated with measured hourly.

weather data (Table 5) are higher than the errors for the mean differences of the measured and simulated temperatures where measured hourly weather data were used (Table 3).

The cumulative probabilities of relative error for the Mississippi data are shown in Fig. 8. Only the probabilities for the ridge position are shown; there were not large differences between the cumulative distributions for the ridge and furrow positions. The relative errors range from -7.5 to 8% and more than 80% of the errors are positive. This is similar to the Washington simulated results. The relative errors are smaller for Mississippi than for the Washington site possibly because the soil temperatures from Mississippi were daily averages and not hourly values.

Soil temperatures simulated using calculated hourly weather data were similar to soil temperatures simulated using measured hourly data except at the higher ranges of soil temperatures. This is partially due to the fact that the early morning and maximum hourly value of radiation near noon are often underestimated. There was more error for surface temperatures than subsurface soil temperatures when calculated hourly data were used as input. This is probably because of the large impact of radiation on surface temperature and evaporation. The impact of radiation is damped for subsurface layers.

Heat energy is also added to the soil with rainfall. When daily weather data are used in models, rainfall data is used as a daily summation, and in 2DSOIL, rainfall and associated heat is added to the soil at night. When hourly measured data are used, rainfall is added at the measurement time. Depending on air temperature, different amounts of heat could be added to the soil. A better estimate heat energy added to the soil with rain for rain during daylight periods may be possible if the temperature of the precipitation was assumed to be the same as the wetbulb temperature rather than as air temperature.

This study has concentrated on use of calculated air temperatures and solar radiation. Hourly wind velocity is also calculated from daily wind runs. High wind

Table 5

Mean differences and standard deviations for simulated temperatures (%) by soil depth at the Washington site where measured and calculated hourly meteorological data were used ($n = 1523$ per depth)^a

Depth (m)	Mean difference (°C)	S.D.
0.00	1.7	2.90
0.08	1.8	2.30
0.15	1.8	2.09
0.25	1.9	2.03
0.38	1.9	2.06
0.53	2.0	2.15
0.69	2.1	2.27
0.84	2.1	2.40
1.07	2.2	2.59
1.37	2.3	2.84
1.68	2.5	3.06

^a The difference was calculated as soil temperatures simulated using measured hourly soil temperatures simulated using calculated hourly meteorological data. S.D. is standard deviation of the differences.

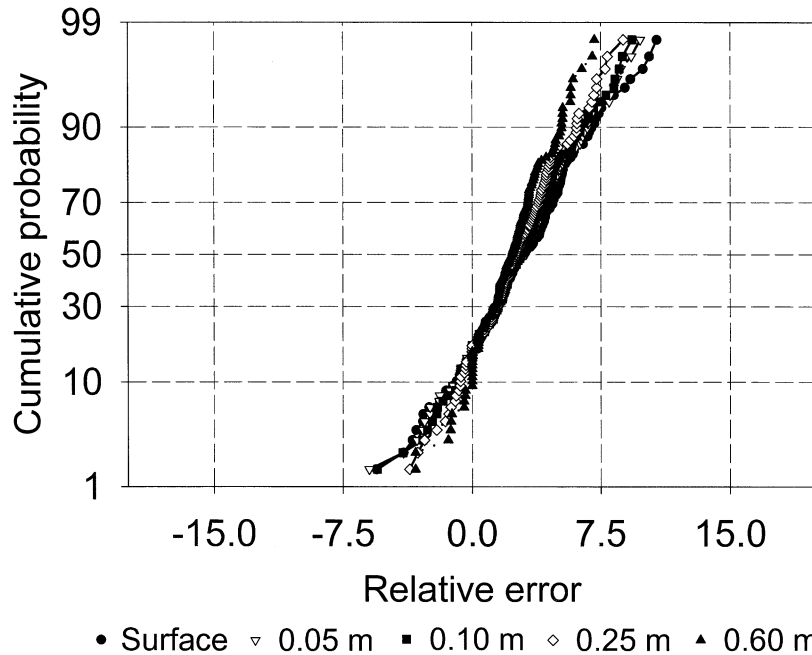


Fig. 8. Cumulative probability distribution of relative errors in simulated soil temperatures at Mississippi for ridge positions using measured and calculated hourly weather data. Relative error is calculated as (simulated with measured hourly–simulated with calculated hourly)/simulated with measured hourly.

velocities can increase evapotranspiration and hence affect soil temperature. The model, however, does account for wind velocity to calculate heat transfer between the soil and air. Inability to model this effectively can lead to additional errors during periods of high wind. This should possibly be addressed in the future.

8. Summary and conclusion

The simulation results and comparison with measured soil temperature data using measured hourly weather data show that 2DSOIL calculates soil temperatures well on bare soil at both sites with low average bias and error. The comparison of simulation and measurements was carried out for a long time sequence of measured values (150 days). The errors were largest during and after rainfall periods where hourly soil temperature values were available. The differences were also largest at the soil surface.

Use of calculated hourly weather data can lead to errors in simulation of soil temperatures. These errors are propagated in the simulation and affect subsurface as well as surface layers temperature simulations. The largest errors were at the surface where there is a boundary between the soil and air. The additional error due to the use of calculated hourly weather data can range from 2 to 3°C This is in addition to

the error of 1–2°C due to the simulation model. Soil temperatures were also under-predicted by 2–3°C when calculated weather data were used. Depending on the purpose of the simulations, this error may be acceptable. The range of errors due to use of calculated weather data is not much larger than the error due to the simulation method and so should be acceptable for many purposes. Spatial variability in soil temperature in a field, however, may be 3–4°C due to variation in irrigation and wind (Yates et al., 1988). This is a similar range in error. If it is important to predict noon or afternoon soil or air temperatures for the purpose of estimating plant stress then measured air temperatures and radiation would be more desirable.

Acknowledgements

The authors gratefully acknowledge the assistance of Dr. Steven Evett and Dr. Jonathan Ephrath who have reviewed earlier versions of this manuscript.

References

- Acock, B.A., Pachepsky, Ya., Timlin, D.J., 2000. Soil-atmosphere Boundary Setting: SetSurf modules. (Chapter 5). In: Timlin, D.J., Pachepsky, Ya., Van Genuchten, M.Th. (Eds.), 2DSOIL, a Modular Simulator of Soil and Root Processes. Remote Sensing and Modeling Laboratory Publication No. 2, USDA Agriculture Research Service, Beltsville, MD.
- Acock, B., Trent, A., 1991. The Soybean Simulator, GLYCIM: Documentation for the Modular Version 91. Agric. Exp. Stn., University of Idaho, Moscow, ID.
- Bowers, S.A., Hanks, R.J., 1965. Reflection of radiant energy from soils. *Soil Sci.* 100, 130–138.
- Budyko, M.I., 1974. *Climate and Life*. Miller, D.H. (Ed., translated). Academic Press, New York.
- Choi, J.S., Fermanian, T.W., Wehner, D.J., Spomer, L.A., 1988. Effect of temperature, moisture, and soil texture on DCPA Degradation. *Agron. J.* 80, 108–113.
- Driedonks, A.G.M. 1981. Dynamics of the Well Mixed Boundary Layer. Scientific Report 81–2, Royal Netherlands Meteorological Institute, De Bilt.
- De Vries, D.A., 1963. Thermal properties of soils. In: van Wijk, W.R. (Ed.), *Physics of the Plant Environment*. North-Holland, Amsterdam, pp. 210–235.
- Ephrath, J., Goudriaan, E.J., Marani, A., 1996. Modelling diurnal patterns of air temperature, radiation, wind speed and relative humidity by equations from daily characteristics. *Agric. Sys.* 51, 377–393.
- Flerchinger, G.N., Saxton, K.E., 1989. Simultaneous heat and water model of a freezing snow-residual-soil system II. Field verification. *Transactions of the ASAE* 32, 573–578.
- Floyd, R.B., Braddock, R.D., 1984. A simple method for fitting average diurnal temperature curves. *Agric. For. Meteorology* 38, 217–229.
- Geng, S., Penning de Vries, F.W.T., Supit, I., 1985. Analysis and simulation of weather variables. II. Temperature and solar radiation. Simulation report CABO-TT No. 5 Wageningen, The Netherlands.
- Khorsandi, F.M., Boone, Y.L., Weerakkody, G., Whisler, F.D., 1996. Validation of the soil temperature subroutine HEAT in the cotton simulation model GOSSYM. *Agron J.* 89, 415–420.
- Koski, A.J., Street, J.R., Danneberger, T.K., 1988. Prediction of Kentucky bluegrass root growth using degree-day accumulation. *Crop Sci.* 28, 848–850.
- Leenhardt, D., 1995. Errors in the estimation of soil water properties and their propagation through a hydrological model. *Soil Use and Management* 11, 15–21.
- Linacre, E.T., 1968. Estimating the net radiation flux. *Agr. Meterol.* 5, 49–63.
- Miller, D.H., 1981. *Energy at the Surface of the Earth*. Academic Press, New York.
- Penman, H.L., 1963. *Vegetation and Hydrology*. C.A.B. Tech. Comm. 53. Commonwealth Agricultural Bureaux, Harpenden, Hertfordshire, UK.

- Robertson, G.W., Russelo, G.A., 1968. Astrometeorological Estimator. Agric. Meteorol. Tech. Bull. 14. Plant Res. Inst., C.E.F. Ottawa 3, Ontario.
- Šimunek, J., Vogel, T., van Genuchten, M.Th., 1994. The SWMS_2D code for simulating water flow and solute transport in two-dimensional variably saturated media. Version 1.2. Res. Rep. 132. United States Salinity Laboratory, Riverside, CA.
- Smithsonian Meteorological Tables. 1963. 6th Edition. Lust, R.J. (Ed.). Smithsonian Institution, Washington, DC.
- Timlin, D.J., 1996. Pachepsky, Ya., Acock, B.A. A design for a modular, generic soil simulator to interface with plant models. *Agronomy J.* 88, 162–169.
- van Genuchten, M.Th., 1980. A closed-form equation for predicting the hydraulic conductivity of unsaturated soils. *Soil Sci. Soc. Am. J.* 44, 892–898.
- Wösten, J.H.M., van Genuchten, M.Th., 1988. Using texture and other soil properties to predict the unsaturated soil hydraulic functions. *Soil Sci. Soc. Am. J.* 52, 1762–1770.
- Weiss, A., 1977. Algorithms for the calculation of moist air properties on a hand calculator. *Trans. A.S.A.E* 20, 1133–1136.
- Yates, S.R., Warrick, A.W., Matthias, A.D., Musil, S., 1988. Spatial variability of remotely sensed surface temperatures at field scale. *Soil Soc. Am. J.* 52, 40–45.